International Journal of Fracture **69:** 51–65, 1994/1995.

Deformation and fracture of Macadamia nuts

Part 1: Deformation analysis of nut-in-shell

CHUN-HUI WANG[1], LIANGCHI ZHANG[2] and YIU-WING MAI[2]
[1] *School of Engineering and Technology, Deakin University, Geelong, VIC 3217, Australia*
[2] *Centre for Advanced Materials Technology, Department of Mechanical and Mechatronics Engineering, University of Sydney, Sydney NSW 2006 Australia*

Received 19 January 1994; accepted in revised form 6 June 1994

Abstract. A theoretical and numerical study of the stress distribution in nutshells being compressed between two rigid plates is presented in Part 1 of this two-part paper. An analytical solution for the contact between a spherical shell and rigid plates has been obtained based on conventional shell theories and Hertz' contact hypothesis, and the results are found to correlate very well with finite element analysis. The effect of the kernel on the deformation and fracture of complete nut-in-shells is also studied using finite element analysis, which shows that the effect of the kernel can be generally ignored as long as the shear modulus of the kernel is lower than that of the shell by two orders of magnitude. A series of tests have been conducted on Macadamia nuts, and the experimental data are discussed in terms of the stress analysis results.

1. Introduction

The phenomenon of the high resistance by some nutshells to fracture has attracted some research attention [1–4]. One such group of nuts is Macadamia nuts that have been successfully cultivated as crops in Australia and the USA. For example, the current production in Australia alone is well over ten thousand tonnes annually. This implies that research into the deformation and fracture mechanisms of the nutshells will not only help in understanding the origin of their high toughness and the structure-property relationship of these biological materials, but also help crack the nuts more efficiently while protecting the kernel from being crushed.

As a biological structure, the nutshell is highly optimized and efficient in terms of strength and toughness due to the ecological evolution and selection. Nutshells are known to possess approximately the same fracture toughness as common ceramics and glass[2], and when compared on the basis of specific strength or modulus (strength or modulus divided by density), Macadamia nuts outperform these materials due to their low density. However, the lack of knowledge of the stress distribution in the shell of a complete nut-in-shell under compression[2] and the lack of appropriate fracture mechanics theory for shells in compression[3] have hindered the progress towards understanding the toughening mechanisms attributing to the high fracture resistance of these nuts.

Jennings and MacMillan[2] conducted a series of experimental studies on the mechanical properties of Macadamia nutshells using C-ring and truncated hemisphere specimens. These results, however, were not related to the fracture of complete nutshells under compression. Recently Vincent[3] studied the fracture behaviour of three different nuts, again, the lack of fracture mechanics theory for shells under compression rendered it difficult to interpret the results.

For Macadamia nuts the typical outer radius (R) is about 12 mm, with the shell thickness (t) being within the range 2 to 4 mm. Although the theoretical solutions for the contact between a solid sphere and rigid plates[5], and the contact between a very thin shell ($R/t \simeq 30$) and rigid plates[6, 7] are known, no work could be found in the literature for the elastic solutions of thick shells compressed between rigid plates. In addition, in the case of nut-in-shell being compressed between rigid plates, the kernel may also affect its deformation and fracture behaviour, should it be in tight contact with the shell.

In general Macadamia nuts have relatively high moisture content [4], about 15–20 percent, when freshly picked ('green'), therefore the kernel is most likely to be in contact with the shell. To reduce the possibility of crushing the kernel when cracking the nut, Macadamia nuts are commonly dried [1] to reduce their moisture contents, typically about 3.5 percent [4], before being subjected to cracking. This normally results in the kernel becoming loose from the shell as the kernel shrinks. While the dried nut can be considered similar to hollow spherical shells, the green nut may be significantly different depending on the properties of the kernel. One extreme case is when the kernel has similar elastic properties to the shell, and in this case a complete nut-in-shell would be equivalent to a solid sphere. It has been reported that the Young's modulus of the Macadamia shell is within the range 4.2 to 5.2 GPa [2, 3], but there is no data available on the mechanical properties of Macadamia kernels.

The objective of Part one of this paper is to determine the distribution of stresses inside the nutshell of a complete nut compressed between rigid plates, so that the results can be applied to explain the fracture behaviour of nut-in-shell under compression. To this end, a theoretical solution based on Hertz' contact theory and the governing equations derived by Reissner[8] was obtained. A finite element analysis was then performed to verify the solution and to study the effect of the kernel. Macadamia nuts were tested by compression between two rigid plates, and the recorded load-deflection curves were later compared with the theoretical and finite element analyses. Macadamia nuts are chosen with a view to help understand the fracture behaviour of this important crop, and hence to improve nut-cracking efficiency. The results, however, can also be applied to other nuts as well.

2. Analysis of nutshell under compression

We first consider the case of dry-in-shell nuts, assuming that the kernel is loose from the shell and does not affect the stress distribution. A schematic drawing of the problem is shown in Fig. 1 together with the spherical coordinates. When the nutshell is subjected to compression, the local contact pressure between the nutshell and the rigid plate is generally not uniform. In the case of extremely thin shells with the radius to thickness ratio exceeding 20:1, Updike and Kalnins [6, 7] demonstrated that the contact load was carried by a line load along the periphery of the contact region. This is primarily due to the combination of large radius-to-thickness ratio and the buckling of the shell under high load.

For Macadamia nuts, however, since the typical radius to thickness ratio is about 6 : 1, buckling of the shell inside the contact region is not likely, especially when the applied load is not very high. Nevertheless, the theories developed for shells assuming that the stress distribution across the wall thickness are composed of direct and bending stresses can still be applied. In analogy to the bending of plates, Reissner [8, 9] obtained a set of solutions for both concentrated and uniformly distributed loads applied at the apex of a shallow shell. However, since the stress distribution is extremely sensitive to the contact pressure distribution (see the stress expressions given in Appendix I), for example, the stresses at the apex are infinite

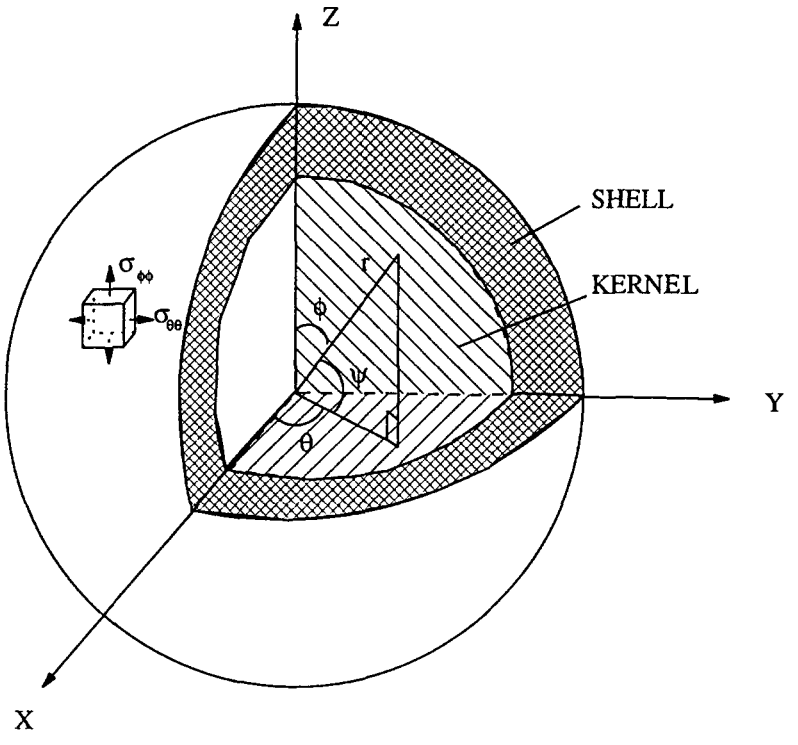

Fig. 1. Schematic drawing of a nut-in-shell and notations of spherical coordinates.

for the concentrated loading case. Therefore it is important to determine the contact pressure distribution in order to estimate the stresses with confidence.

To determine the contact radius and the pressure distribution between a shell and a rigid plate in contact, the displacement due to a point load is required. Here the Macadamia nutshell is assumed to be isotropic (see Part 2 of this paper), hence the simple solution obtained by Reissner [9] is considered,

$$w = -\frac{\sqrt{12(1-\nu^2)}}{2\pi}\frac{PR}{Et^2}\,\mathrm{kei}\left(\frac{r}{l}\right), \tag{1}$$

where ν is the Poisson's ratio and the variable r denotes the distance from the Z axis (see Fig. 2, in which the different definition of the Z axis from that of Reissner is the reason for the negative sign in the above equation), and function $\mathrm{kei}(x)$ is a Bessel function [10]. The constant l is equal to $\sqrt{Rt}/\sqrt[4]{12(1-\nu^2)}$. For small argument values ($x < 5.0$) the function $\mathrm{kei}(x)$ can be expressed by

$$\mathrm{kei}(x) = -\tfrac{1}{4}\pi + 0.143x + 0.261x^2 - 0.137x^3 + 0.0256x^4 - 0.0017x^5, \tag{2}$$

which has been obtained by fitting the tabulated data listed in [10]. Also we have

$$\alpha - w_1(\eta) = z_1 \equiv \frac{\eta^2}{R + \sqrt{R^2 - \eta^2}}, \tag{3}$$

where η is the distance between the origin and an arbitrary point inside the contact area, and α is the approach [5] between the shell and the rigid plate, which is also the change in the radius of the complete shell. Although (1) was obtained for the case of a concentrated load applied at the apex of the shell, it is considered applicable to the present case as the contact is over a relatively small region compared with both the shell's radius R and thickness t. Therefore equation (3) can be rewritten as,

$$\alpha = -\int\int \frac{\sqrt{12(1-\upsilon^2)}}{2\pi}\frac{R}{Et^2}\,\mathrm{kei}\left(\frac{s}{l}\right) q(r)s\,\mathrm{d}s\,\mathrm{d}\psi + \frac{\eta^2}{R+\sqrt{R^2-\eta^2}}, \tag{4}$$

where $s = (r^2 + \eta^2 - 2r\eta\cos\theta)^{1/2}$, see Fig. 2, $q(r)$ is the pressure distribution, and the integration is performed over the contact area. Inserting (2) in (4) we have

$$\alpha = \frac{\sqrt{3(1-\upsilon^2)}PR}{4Et^2} - \int\int F(s)q(r)\,\mathrm{d}s\,\mathrm{d}\psi + \frac{\eta^2}{R+\sqrt{R^2-\eta^2}}, \tag{5}$$

where

$$F(s) = \frac{Rs\sqrt{3(1-\nu^2)}}{\pi Et^2}\left[\mathrm{kei}\left(\frac{s}{l}\right) + \frac{\pi}{4}\right]. \tag{6}$$

The correct contact radius (r_p) for a given contact load should be such that the approach (α) is constant for any η between 0 and r_p. Since $\mathrm{kei}(s/l) + \frac{1}{4}\pi$ is very small for $r \in [0, r_p]$ (e.g. in the present case we have $s/l \leqslant 2r/l \simeq r/1.5$), the first term in the above equation effectively gives a first order approximation for approach α,

$$\alpha = \frac{\sqrt{3(1-\upsilon^2)}PR}{4Et^2}. \tag{7}$$

To satisfy (5) for any $\eta \in [0, r_p]$, the second term of the right side of that equation should be proportional to η^2. In the case of contact between solid bodies, $F(s)$ is constant[5], hence an explicit expression of the contact radius can be obtained. This is, however, impossible in the present case due to the complex nature of the Bessel function involved. Nonetheless, (5) can be solved numerically to determine the contact radius. Here we shall consider elastic loading only, and assume that the contact pressure distribution follows Hertz' assumption: spherical distribution over the contact area. Denoting the total applied load as P, distributed over a circular area of radius r_p, as indicated in Fig. 2, the contact pressure, $q(r)$, can be expressed as

$$q(r) = k\sqrt{r_p^2 - r^2}, \tag{8}$$

where $k = 3P/2\pi r_p^3$. For a given contact load P, since the last two terms on the right side of (5) are very small compared with the first term, and both are functions of η, this means the contact radius is the solution to the following equation

$$G(\eta) \equiv -\int_0^{2\pi}\int_0^{\eta} \frac{R\sqrt{3(1-\nu^2)}}{\pi Et^2}\left[\mathrm{kei}\left(\frac{s}{l}\right) + \frac{\pi}{4}\right] q(r)r\,\mathrm{d}r\,\mathrm{d}\theta + \frac{\eta^2}{R+\sqrt{R^2-\eta^2}} = 0. \tag{9}$$

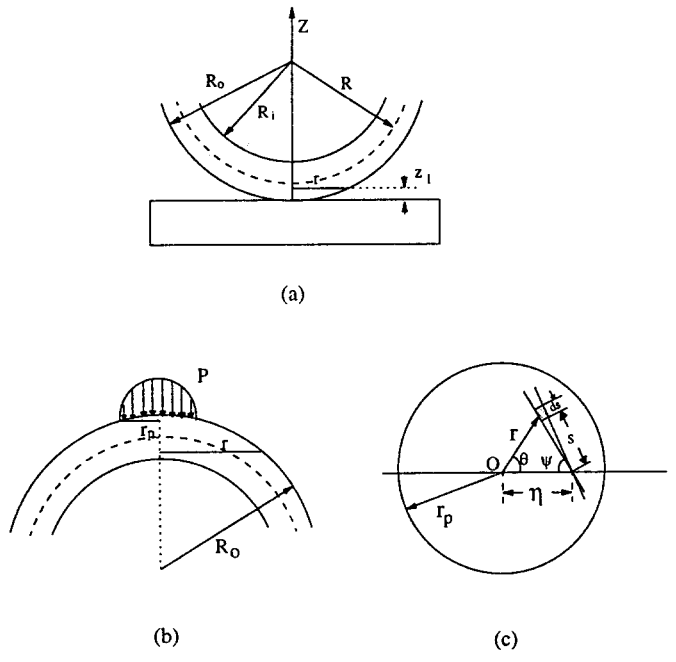

Fig. 2. The coordinates before and after compression for a point on the contact surface.

Function $G(\eta)$ is a measure of the separation between the shell and the rigid plate, and the boundary of the contact region is obviously defined by $G(r_p) = 0$, with positive $G(\eta)$ corresponding to separation between shell and plate. This equation can be solved by iteration or Newton–Raphson's method. An example is shown in Fig. 3, which demonstrates that the convergence is rapid. Therefore the contact radius can be readily obtained from the following iteration equation

$$r_p = \left[\left(R + \sqrt{R^2 - r_p^2}\right) \int_0^{2\pi} \int_0^{r_p} \frac{R\sqrt{3(1-\nu^2)}}{\pi E t^2} \left[\mathrm{kei}\left(\frac{s}{l}\right) + \frac{\pi}{4}\right] q(r) r \, \mathrm{d}r \, \mathrm{d}\theta\right]^{0.5}. \quad (10)$$

For an initial guess value (r_p) of 12 mm, which represents the maximum possible value for a shell radius $R = 12$ mm, three iterations would suffice for an accuracy of 1 percent in terms of the contact radius. The stresses and deflection due to the contact pressure can now be obtained by integrating those due to a concentrated load. Since this will involve cumbersome numerical integrations, a simpler alternative would be to utilize the solutions in [9] for a uniformly distributed load. Here we assume the spherically distributed contact load can be simulated by a uniform distribution load with an average contact pressure,

$$\bar{q} = P/\pi r_p^2, \quad (11)$$

where the contact radius r_p is that obtained from (9). The stress expressions are derived in Appendix I, which also corrects a few errors made in [9].

The above analyses are only for the case of a hollow spherical shell, or the case of a nut-in-shell with the kernel being loose from the shell. In other words, no effect of the kernel has been taken into account. Since the kernel in general has different material properties from

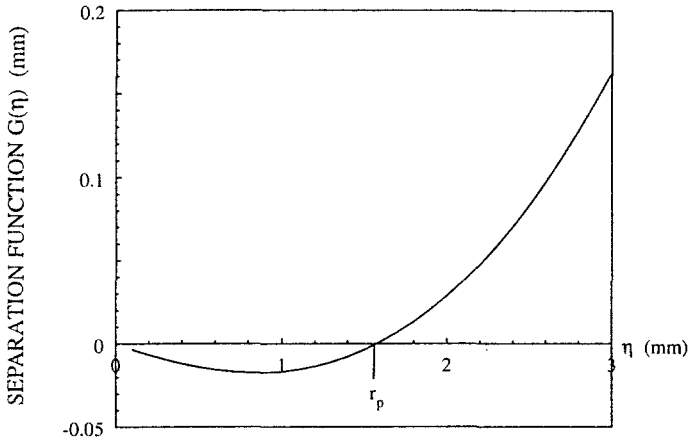

Fig. 3. Separation function $G(\eta)$ versus contact radius.

the shell, analytical solutions for a nut-in-shell with the kernel being in contact with the shell would be difficult. However, since the kernel is much softer than the shell, it is believed that the effect of the kernel can be ignored. To examine the above hypothesis and to verify the above analytical solutions, a finite element analysis has been carried out, which is discussed in the next section together with experimental results on whole Macadamia nuts.

3. Finite element analysis and experiments

Since the contact between a shell and two rigid plates is an axisymmetrical loading problem, only a quarter needs to be considered. Finite element analysis package ABAQUS [11] was used in the present work, and an eight-noded axisymmetrical element was adopted throughout. The inner and outer radii of the shell are 10 and 12 mm, respectively, with the shell thickness being 2 mm, which is the minimum shell thickness. About 600 elements were used for this particular configuration and geometry. Special interface elements [11] provided by the software were used to model the contact between the shell and the rigid plates.

Both the shell [2] and kernel are considered as being isotropic, and the elastic data ($E = 5.2$ MPa, $\nu = 0.3$) for shells, taken from [2], are also in good agreement with the data obtained by the present authors (see Part 2 of this paper). Due to the lack of data on Macadamia kernels, four different Young's moduli are examined in this work to evaluate to what degree the kernel will affect the stress distributions in the shell. The kernel's Young's modulus is taken to be 0.001, 0.01, 0.1 and 1.0 times that of the shell, respectively. Moreover, three Poisson's ratios, 0, 0.5, and 0.25, which correspond to the kernel being extremely compressible, incompressible, and similar to the shell, respectively, are also studied.

A peak deflection of 1.0 mm between poles of a whole nut is used to simulate displacement-controlled loading, which in the case of a hollow spherical shell corresponds to a contact load of about 2 kN. This is considered appropriate for Macadamia nuts as it has been reported [2, 3] that the load required to crack both 'green' and 'dried' nuts is lower than this value. In this case the contact radius from FE analysis is about 1.78 mm whereas that calculated from (9) is 1.58 mm, exhibiting a good correlation. Further discussion will be presented in the next section.

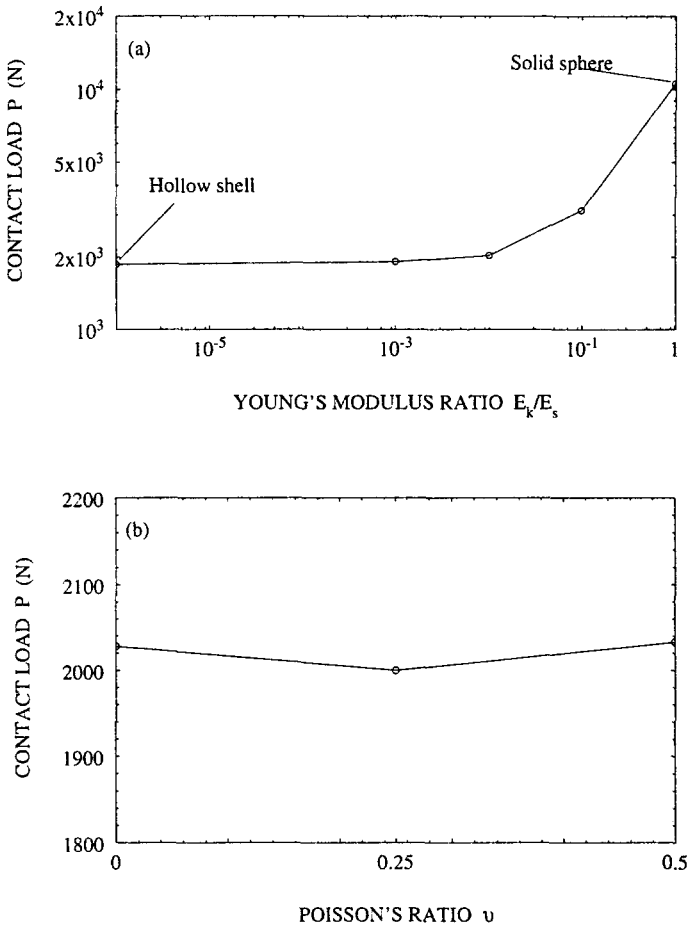

Fig. 4. Effect of kernel's mechanical properties on the deformation of nut-in-shell in terms of contact load required for a given deflection of 1 mm; (a) Young's modulus with $\nu = 0.3$, and (b) Poisson's ratio.

Experiments were conducted on whole Macadamia nuts in slow compression between two rigid plates, and the load and deflection data were recorded using a computer data logging system. The mean diameter was estimated by averaging the diameters measured in the x, y, and z directions. The average shell thickness measured after fracture is about 2 mm. It is interesting to note that when fracture occurred the nuts did not suddenly break into pieces, and the partially fractured nuts were still able to support a load. The shell was generally incompletely fractured with one main crack running between loading points. Further compression was necessary after the main fracture to break up the nut completely.

4. Results and discussion

A comparison of the results from theoretical analysis, finite element calculations, and experiments is presented below, which serve as a basis for the analysis of the fracture of nut-in-shells.

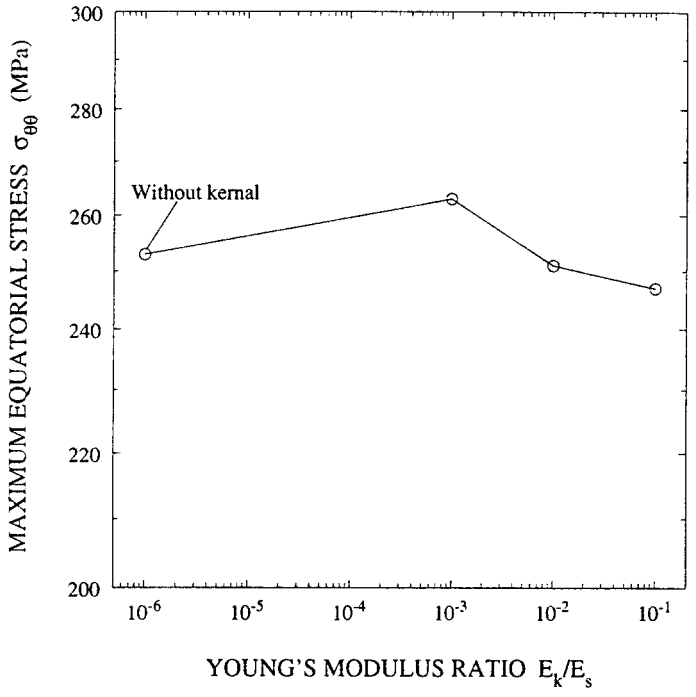

Fig. 5. Effect of Young's modulus ratio on the maximum equatorial stress $\sigma_{\theta\theta}$.

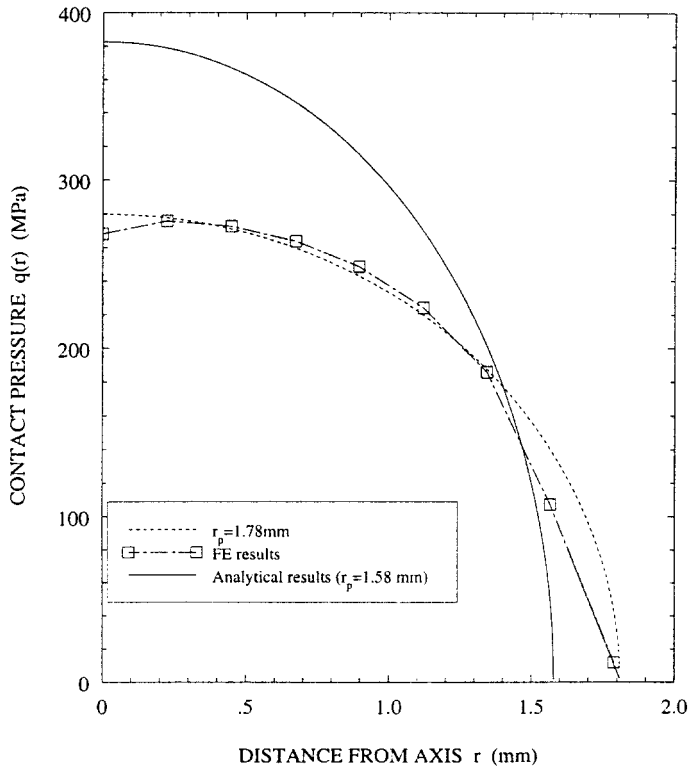

Fig. 6. Contact pressure distributions from analytical calculations and finite element analysis.

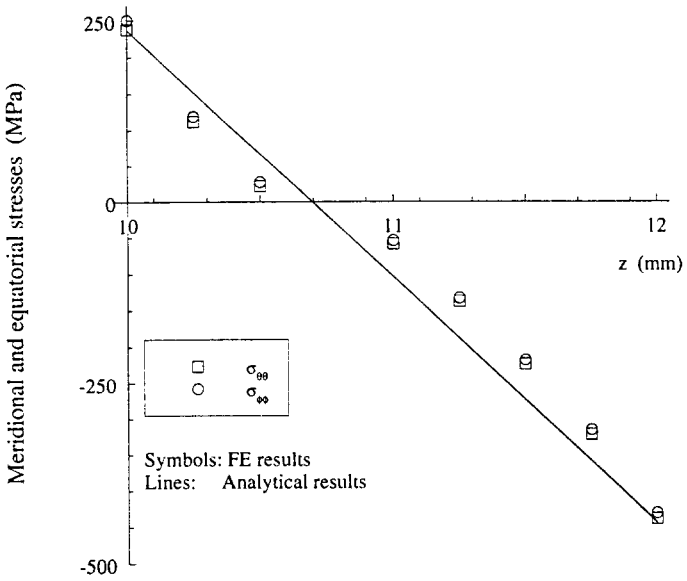

Fig. 7. Distribution of meridional and equatorial stresses across shell thickness of a hollow spherical shell.

4.1. Effects of kernel

When the kernel is in close contact with the shell, it may affect the stress distribution in complete nuts by increasing the resistance to deformation. An example of the finite element analysis is shown in Fig. 4(a), in which the contact load to produce a deflection of 1 mm between contact points is plotted against the Young's modulus ratio. Here E_k and E_s represent the Young's modulus of kernel and shell, respectively. With increasing Young's modulus of the kernel, the load level required to produce the same deformation of the nut increases, especially when the kernel's elastic modulus approaches that of the shell. A maximum of five times increase occurs when the kernel has the same elastic properties as the shell, although this is not very likely in reality. In the present work, the Young's modulus of the Macadamia kernel is estimated to be about one-hundredth that of the shell. Hence, according to the finite element analysis, the effect of the kernel's Young's modulus can be ignored. It should be pointed out that to enable valid comparisons, the same Poisson's ratio of 0.3 was used in the finite element modeling.

Since Macadamia kernels have a very high percentage of oil [4], they can be considered as an incompressible material. This implies that the Poisson's ratio may be close to 0.5. To examine the influence of the compressibility of the kernel (which is measured by $(1-2\nu)/E$) on the deformation behaviour of the nut-in-shells, finite element analyses were performed for three different Poisson's ratios, 0, 0.25, and 0.5. The results are shown in Fig. 4(b), and it can be seen that the compressibility of the kernel has little effect, this is primarily due to the very small change of the space inside the nut when compressed, so that the kernel can readily alter its shape to accommodate this small change of shape of the shell.

Therefore, it is concluded that the kernel has little effect on the deformation behaviour of the nut-in-shells. This implies that the methods developed for hollow spherical shells can be applied to complete nuts-in-shells. This is further demonstrated by Fig. 5, in which the maximum equatorial stress in the shell beneath the loading point is plotted against the ratio

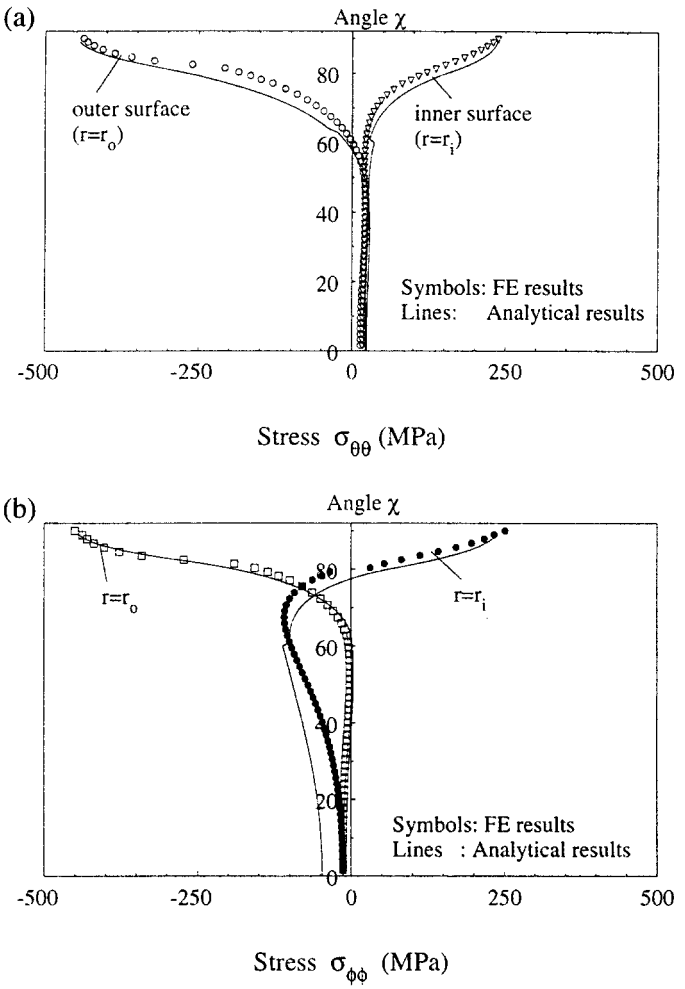

Fig. 8. Distribution of (a) meridian and (b) equatorial stress on inner and outer surfaces of the shell.

of the Young's modulus. It can be seen that the maximum equatorial stress (tensile) is almost constant for a large range of Young's moduli of the kernel.

4.2. Comparison of Theory and Finite Element Analysis

The contact pressure distribution is critical in determining the stress distribution inside the shells, at least the contact radius, as can be seen from Appendix I. Since in the present work we adopted Hertz' assumption, it is important to compare the distribution calculated from (8) with that obtained from finite element analysis. An example is shown in Fig. 6, where the total contact load is 2 kN. This figure demonstrates that the contact pressure obeys the spherical distribution assumption, which is very different from the case of a thin shell studied in [7]. The solid curve represents that calculated from (8), whereas the chained curve with different symbols represents the finite element results. The overestimation of the maximum contact pressure is due to the difference in the calculated contact radius, and when the contact radius obtained from finite element analysis is used, the calculated contact pressure distribution (shown by the dotted curve in Fig. 6) gives good agreement with finite element analysis. It

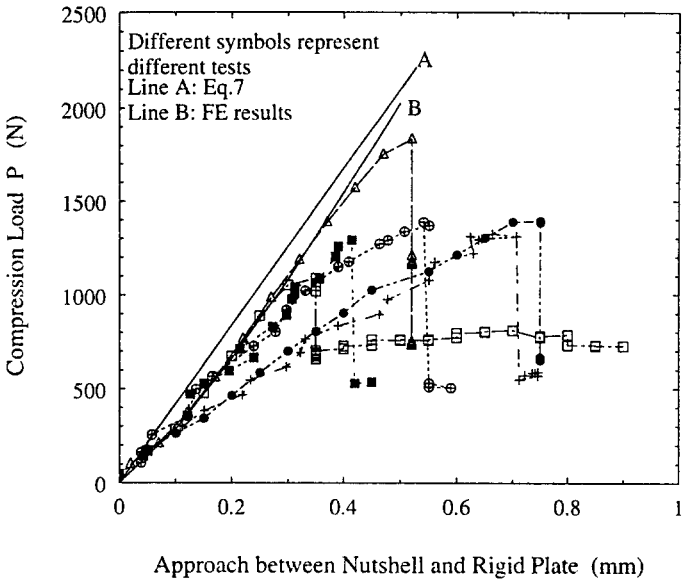

Fig. 9. Comparisons between finite element calculations, analytical results and experimental data for nuts-in-shells under compression.

should also be pointed out that the accuracy of the present method is to some extent dependent on that of the solution (1) for the shell's deflection under a point load.

One assumption made in deriving the governing equations [8] was that the stresses (meridional and equatorial) in the shell can be considered as the sum of the direct stresses (uniform across wall thickness) and pure bending stresses. This is basically a thin shell assumption, and it is not certain that this assumption is still valid for a radius to thickness ratio between 5:1 to 6:1, as in the present case. To this end, the distribution of the meridian ($\sigma_{\phi\phi}$) and equatorial ($\sigma_{\theta\theta}$) stresses just beneath the loading point are plotted in Fig. 7 with respect to the position. Clearly the distribution of meridional and equatorial stresses do not exhibit exact linearity, but the deviation is relatively small. Moreover, the maximum stress levels calculated from the theories agree very well with the finite element analysis.

It is also observed that the maximum stresses occurred right beneath the loading point, with the maximum compressive stress being on the outer surface and the maximum tensile stress on the inner surface. Since Macadamia nut shells have better resistance to compression than tension, as most wood materials do, their fracture is controlled by the tensile stress (in particular equatorial component). Figures 8(a) and (b) compare the distributions of the equatorial and meridian stresses on the inner and outer surfaces, where the symbols represent the finite element results and solid curves the theoretical results. It can be seen that the correlation is satisfactory, especially for the equatorial stress, the driving force for the initiation and propagation of cracks leading to nutshell failure.

4.3. Fracture of Macadamia nuts under compression

Typical experimental load-deflection curves for nuts compressed between two rigid plates are shown in Fig. 9, where different symbols represent different samples. Curve B is calculated from the finite element analysis and curve A is obtained from (5). There is reasonable agreement between the computed curves and some of the experimental curves in the elastic

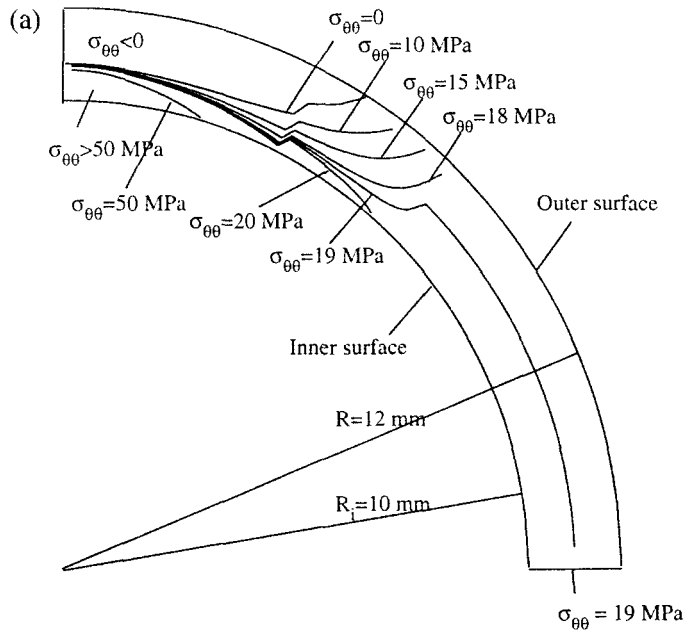

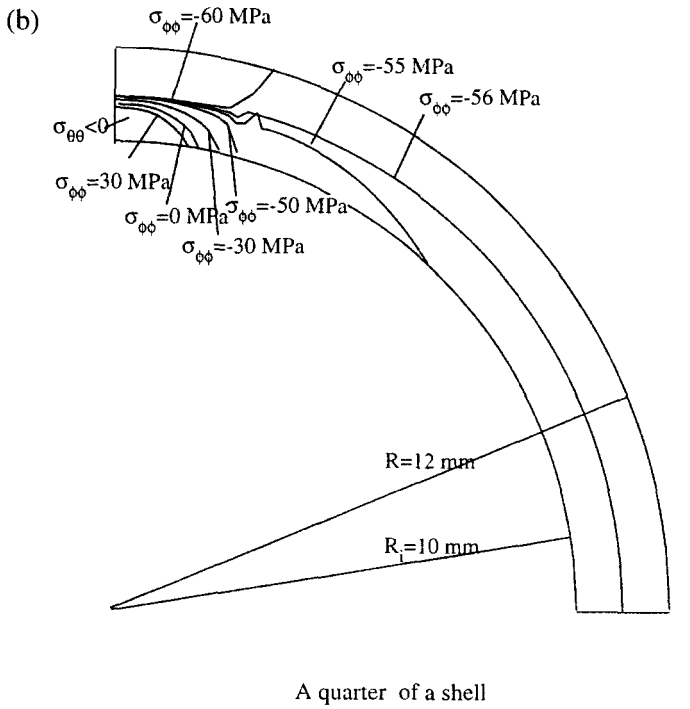

Fig. 10. A map of (a) the equatorial stress distribution and (b) merdional stress distribution in a shell under compression.

deformation region. It can also be seen that the partially fractured nuts can still support about half of the peak load, and a considerable amount of further compression would be needed to fully crack the nut.

The tensile strength of Macadamia nut shells is about 40–50 MPa [2], but the maximum tensile stress generated in the inner layer of the shell under compression at fracture is typically about 188 MPa (corresponding to a total contact load of 1.5 kN); an example of the equatorial stress distribution is shown in Fig. 10(a). Hence cracks must have initiated on the inner surface of the wall, but the compressive direct stress across the wall thickness prevents the crack from penetrating the shell, since the driving force is decreasing rapidly and eventually drops below zero as cracks propagate from the inner surface to the outer surface. Hence extra load is required to extend the crack further on the inner surface, and only when the total driving force reaches the fracture toughness of the material, which is reported to be $1.8\,\mathrm{MPa}\sqrt{m}^{1/2}$ [2], can the cracks break through the shell and form the main crack. However, due to the compressive direct stress under the loading point, which is perpendicular to the crack plane, cracks still cannot pass through the contact point. This is why nuts do not fracture completely and can still support some load after the main fracture.

The meridional stress, as shown in Fig.10(b), which is compressive except in a small region underneath the loading point, also accounts for the stability of the nuts under compression. As long as the shell material is capable of sustaining a relatively high compression load, the nuts will not crack equatorially.

5. Conclusion

A solution for the contact between a spherical shell and rigid plates has been obtained, which is verified by finite element analysis. It is shown that the analytical solution is also applicable to the case of nut-in-shells under compression, provided the kernel is soft with shear modulus being less than one-hundredth that of the shell. The Poisson's ratio of the kernel is found to have little effect upon the stress distribution or the shear modulus of the kernel, provided it is less than one-tenth that of the shell.

The high toughness and incomplete fracture behaviour of nuts under compression can be explained in terms of the stress distribution in the shell. While the tensile equatorial stress acting on the inner surface of the shell is responsible for the initiation of cracks, the compressive direct stress across the wall thickness deters crack propagation.

Appendix I

Consider the case of a spherical shell under a uniformly distributed load (P) over an area of radius of r_p. Denote $x = r/l$, then the direct stresses can be derived using a similar method as reported in [9]. Since a few errors have been found in that publication (Eqns. (64a), (64b), and (68)), the correct forms are presented here

$$\sigma_{\phi\phi,D} = \frac{PR}{\pi t r_p^2} \begin{cases} c_1 \frac{\mathrm{bei}' x}{x} - c_2 \frac{\mathrm{ber}' x}{x} - \frac{1}{2} & r \leqslant r_p \\ c_3 \frac{\mathrm{kei}' x}{x} - c_4 \frac{\mathrm{ker}' x}{x} - \frac{1}{2}\left(\frac{r_p}{r}\right)^2 & r > r_p \end{cases}, \tag{A1}$$

$$\sigma_{\theta\theta,D} = \frac{PR}{\pi t r_p^2} \begin{cases} c_1\,\mathrm{bei}'' x - c_2\,\mathrm{ber}'' x - \frac{1}{2} & r \leqslant r_p \\ c_3\,\mathrm{kei}'' x - c_4\,\mathrm{ker}'' x + \frac{1}{2}\left(\frac{r_p}{r}\right)^2 & r > r_p \end{cases}. \tag{A2}$$

And the bending stresses on the inner and outer surfaces are

$$\sigma_{\phi\phi,B} = H \begin{cases} -c_1\left(\text{bei}\, x + \frac{1-\nu}{x}\text{ber}''\, x\right) + c_2\left(\text{ber}\, x - \frac{1-\nu}{x}\text{bei}'\, x\right) & r \leqslant r_p \\ -c_3\left(\text{kei}\, x + \frac{1-\nu}{x}\text{ker}'\, x\right) + c_4\left(\text{ker}\, x - \frac{1-\nu}{x}\text{kei}'\, x\right) & r > r_p \end{cases}, \tag{A3}$$

$$\sigma_{\theta\theta,B} = H \begin{cases} -c_1\left(\nu\,\text{bei}\, x - (1-\nu)\frac{\text{ber}'\, x}{x}\right) + c_2\left(\nu\,\text{ber}\, x + (1-\nu)\frac{\text{bei}'\, x}{x}\right) & r \leqslant r_p \\ -c_3\left(\nu\,\text{kei}\, x - (1-\nu)\frac{\text{ker}'\, x}{x}\right) + c_4\left(\nu\,\text{ker}\, x + (1-\nu)\frac{\text{kei}'\, x}{x}\right) & r > r_p \end{cases}, \tag{A4}$$

where variable r is equal to $R\sin\phi$ at the outer surface and

$$H = \frac{\mp 6PR}{\pi t r_p^2 \sqrt{12\,(1-\nu^2)}}. \tag{A5}$$

The parameter H takes a negative sign for outer surface, and constants c_n are given by

$$c_1 = -\mu\text{ker}'\mu, \quad c_2 = \mu\text{kei}'\mu, \quad c_3 = -\mu\text{ber}'\mu, \quad c_4 = \mu\text{bei}'\mu, \quad c_5 = -1, \tag{A6}$$

where $\mu = r_p/l$. Here ber, bei, ker, and kei, are the four Bessel functions, whose values are available in tabulated form [10]. Other constants are as defined in the text.

The normal displacement of the shell is,

$$w = \begin{cases} C_1\text{ber}\, x + C_2\,\text{bei}\, x + C_5 & 0 < r \leqslant r_p \\ C_3\,\text{ker}\, x + C_4\,\text{kei}\, x & R > r > r_p \end{cases}, \tag{A7}$$

where constants C_n are defined by

$$C_n = c_n \frac{PR^2\sqrt{12(1-\upsilon^2)}}{\pi E t r_p^2}. \tag{A8}$$

Clearly the contact radius r_p is crucial to the determination of both the deflection (w) and stresses ($\sigma_{\phi\phi}$, $\sigma_{\theta\theta}$) for a given load.

Acknowledgment

The authors acknowledge Premier Nuts Australia, Lismore, New South Wales, Australia, for providing Macadamia nuts used in the present work. Finanical support by a Sydney University Research Grant is much appreciated. We also thank J.F.V. Vincent for helpful discussions and useful suggestions for experiments on the nuts.

References

1. Y. Sarig, F. Grosz, and S. Rasis, *Journal of Agriculture and Engineering Research* 25 (1980) 367–374.
2. J.S. Jennings and N.H. Macmillan, *Journal of Materials Science* 21 (1986) 1517–1524.
3. J.F.V. Vincent, in *Proceedings of the Materials Research Society Fall Meeting* (1992).
4. J.G. Woodroof, *Tree Nuts, Production, Processing, Products*, Vol.1, AVI Publishing Company, Westport, Connecticut (1967).

5. S.P. Timoshenko and J.N. Goodier, *Theory of Elasticity*, 3rd edn., McGraw-Hill Book Company, New York (1970).
6. D.P. Updike and A. Kalnins, *Journal of Applied Mechanics* 37 (1970) 635–640.
7. D.P. Updike and A. Kalnins, *Journal of Applied Mechanics* 39 (1972) 1110–1114.
8. E. Reissner, *Journal of Mathematical Physics* 25 (1946) 80–85.
9. E. Reissner, *Journal of Mathematical Physics* 25 (1946) 279–300.
10. H.R. Dwight, *Tables of Integrals and Other Mathematical Data*, 4th edn., The Macmillan Company, New York (1964) 201.
11. *ABAQUS User's Manual*, Version 4.8, Hibbitt, Karlsson and Sorensen, Inc. (1989).